THE JOURNAL OF BIOLOGICAL CHEMISTRY VOL. 291, NO. 45, pp. 23532–23544, November 4, 2016

The MicroRNA miR-191 Supports T Cell Survival Following Common γ Chain Signaling*[S]

Received for publication, May 31, 2016, and in revised form, August 15, 2016 Published, JBC Papers in Press, September 15, 2016, DOI 10.1074/jbc.M116.741264

Erik Allen Lykken and Qi-Jing Li[1]

From the Department of Immunology, Duke University Medical Center, Durham, North Carolina 27710

To ensure lifelong immunocompetency, naïve and memory T cells must be adequately maintained in the peripheral lymphoid tissues. Homeostatic maintenance of T cells is controlled by tonic signaling through T cell antigen receptors and common γ chain cytokine receptors. In this study, we identify the highly expressed microRNA miR-191 as a key regulator of naïve, memory, and regulatory T cell homeostasis. Conditional deletion of miR-191 using LckCre resulted in preferential loss of peripheral CD4$^+$ regulatory T cells as well as naïve and memory CD8$^+$ T cells. This preferential loss stemmed from reduced survival following deficient cytokine signaling and STAT5 activation. Mechanistically, insulin receptor substrate 1 (Irs1) is a direct target of miR-191, and dysregulated IRS1 expression antagonizes STAT5 activation. Our study identifies a novel role for microRNAs in fine-tuning immune homeostasis and thereby maintaining the lymphocyte reservoir necessary to mount productive immune responses.

Adaptive immunity hinges upon a naïve lymphocyte pool that is sufficient in size and breadth to enable Darwinian selection of clones responsive to foreign antigens. Additionally, the generation and maintenance of memory lymphocytes is required for rapid clearance responses against repeated insult. Age-accelerated loss of thymic output post-puberty reduces the T lymphocyte input necessary for peripheral protection and thus highlights the importance of maintaining pools of both naïve and memory T lymphocytes.

Much work has addressed the longevity of naïve and memory cell pools (1, 2) as well as the pro-survival signals that maintain resting T cells in the periphery. Naïve and memory T cells have different strategies and requirements for long-term survival. Naïve T cells, especially naïve CD8$^+$ T cells, are maintained *in vivo* with minimal proliferation and require tonic signaling through the T cell antigen receptor (TCR)[2] (3) as well as the cytokine IL-7 (4). Naïve CD4$^+$CD25$^+$ regulatory T cells (T_{Regs}) also require tonic TCR signaling but shift in cytokine dependence toward IL-2 (5). Memory cells are more frequently found in the cell cycle, and their maintenance depends much less on TCR signaling (6). Instead, they rely primarily on cytokine signals, namely IL-7 and IL-15, although IL-15 is thought to be more important for proliferation than survival (7, 8). Given limited sources of pro-survival cytokines, naïve, memory, and regulatory T lymphocytes are constantly competing for survival. Thus, the efficiency of responses to these specific and limited pro-survival cytokines is essential for maintaining T lymphocytes at homeostasis.

On the surface of T lymphocytes, the pro-survival cytokines IL-7, IL-2, and IL-15 engage with receptors sharing a common subunit: the common γ chain (CD132). This leads to signaling convergence through a shared mechanism, creating a recipe for systemic collapse of adaptive immunity following major perturbation of the pathway. Such systemic collapse is seen in SCID, which arises from the loss of key components required to maintain resting T lymphocytes (*e.g.* CD127, CD132, and JAK3) (9). However, small perturbations seem unlikely to collapse the system, instead merely forcing it toward a new equilibrium. Such perturbations are unlikely to present as striking clinical immunodeficiency but may still have serious implications for immunity throughout the life of a patient and influence the outcome of immunotherapies. As such, investigation into the mechanisms by which the immune system fine-tunes the maintenance of resting T lymphocytes may provide new insights to diagnose minor immunodeficiencies and offer new approaches for therapies to promote immunocompetency throughout the life of the patient.

One such mechanism for finely tuning T lymphocyte activity is executed by microRNAs (miRNAs), a population of small (~22 nucleotide) non-coding RNAs, that guide the RNA-induced silencing complex to modulate protein levels by binding to and thereby preventing target mRNA translation (10, 11). Many recent studies have highlighted important roles for miRNAs in T lymphocytes, including modulation of TCR signal strength (12), effector cell survival (13), differentiation (14, 15), and function (16, 17). However, there have been no studies that describe the role miRNAs play in the survival of resting T lymphocytes. Here we present data that demonstrate the role of the highly expressed miRNA miR-191 in supporting the survival of naïve, memory, and regulatory T lymphocytes.

Results

miR-191 Promotes T Cell Survival Following TCR Stimulation—A recent study that quantified miRNA expression among immune cell subsets revealed the presence of select miRNA species with high expression across T and B lympho-

* This work was supported by American Diabetes Association Grant 1–10-JF-28 and National Institutes of Health Grant R01AI091878 (to Q. J. L.). The authors declare that they have no conflicts of interest with the contents of this article. The content is solely the responsibility of the authors and does not necessarily represent the official views of the National Institutes of Health.

[S] This article contains supplemental Table 1.

[1] To whom correspondence should be addressed: Dept. of Immunology, Duke University Medical Center, Box 3010, Durham, NC 27710. Tel.: 919-668-4070; E-mail: qi-jing.li@dm.duke.edu.

[2] The abbreviations used are: TCR, T cell receptor; T_{Reg}, CD4$^+$ regulatory T cell; miRNA, microRNA; DC, dendritic cell; DPBS, Dulbecco's phosphate buffered saline; EdU, 5-ethynyl-2′-deoxyuridine; ESC, embryonic stem cell; MACS, magnet-assisted cell sorting; MFI, mean florescence intensity; RT-qPCR, RT quantitative PCR; Tricine, *N*-[2-hydroxy-1,1-bis(hydroxymethyl) ethyl]glycine.

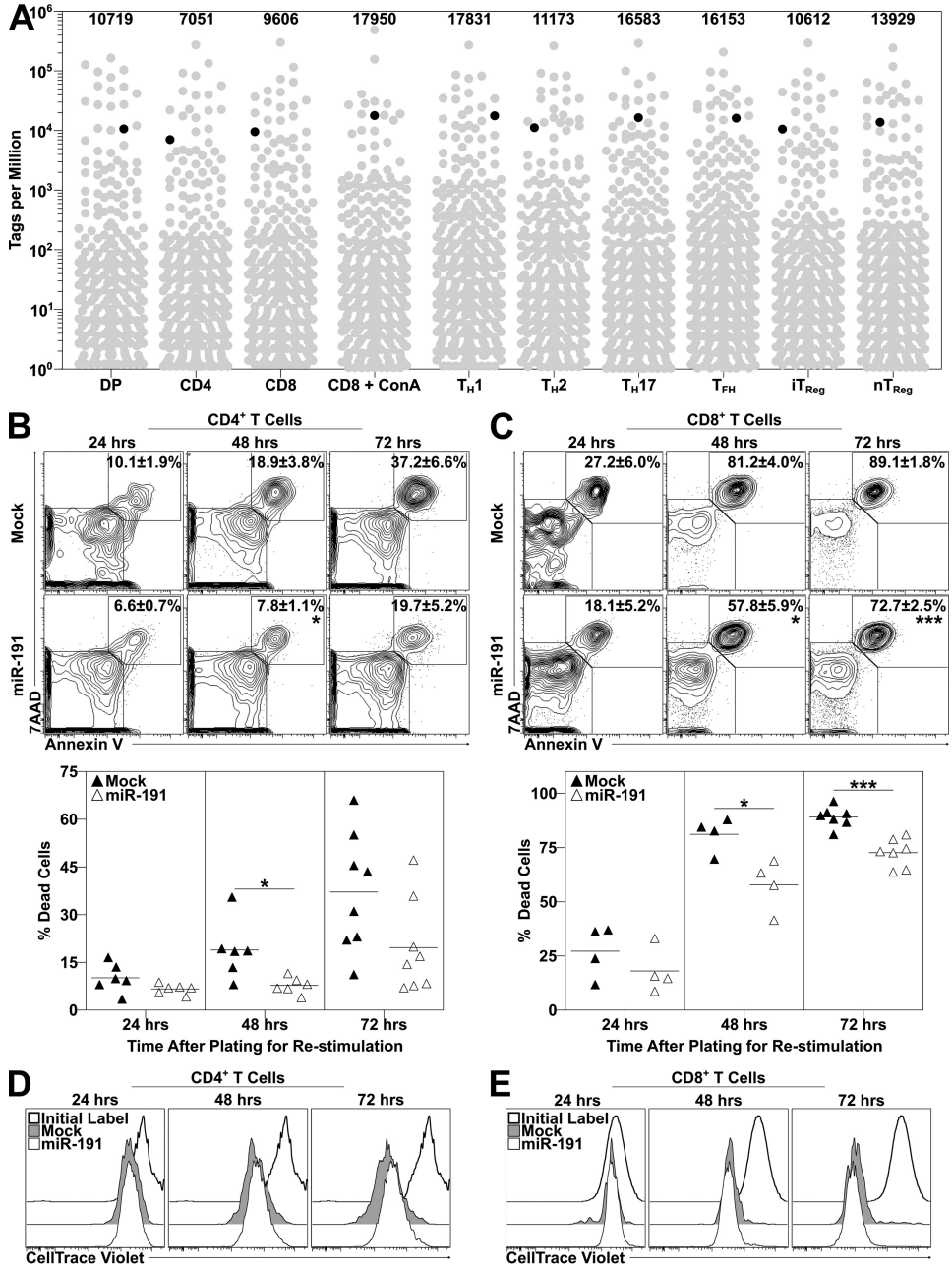

FIGURE 1. **The highly expressed miRNA miR-191 enhances T cell survival.** *A*, plot of reads from microsequencing of small RNAs for various T cell subsets from supplemental data provided in Ref. 18. Each miRNA with greater than 1 tag per million in a given sample is plotted as a *gray dot*. miR-191 is plotted as a *black dot*, and the tag per million value for miR-191 is given for each cell type plotted. *B–E*, $CD4^+$ and $CD8^+$ T cells were purified by MACS, infected with mock-GFP or miR-191-GFP retrovirus, restimulated for 24 h post-infection with plate-bound α-CD3ϵ/CD28, and analyzed at the indicated times post-plating by flow cytometry. *B* and *C*, Annexin V and 7-Aminoactinomycin D staining of GFP^+CD4^+ and GFP^+CD8^+ T cells. *Top panels*, representative contour plots. *Bottom panels*, summary data. *D* and *E*, representative MFI plots for CellTrace Violet levels in live, GFP^+ cells. Data were derived from two to three independent experiments ($n = 4–8$/group). Differences in group means were determined by unpaired Student's *t* test: *, $p < 0.05$; ***, $p < 0.001$.

cyte differentiation pathways (18). The consistently elevated expression of these miRNAs among all lymphocytes suggests that these miRNAs play a fundamental role in lymphocyte biology. Although the majority of these highly expressed miRNAs belong to the well studied let-7 family, one miRNA remains uncharacterized: miR-191 (Fig. 1*A*). To determine the significance of miR-191 expression in T lymphocytes, wild-type murine $CD4^+$ and $CD8^+$ T cells were retrovirally induced to overexpress miR-191. Both $CD4^+$ and $CD8^+$ T cells overexpressing miR-191 were protected from activation-induced cell death (Fig. 1, *B* and *C*); no significant differences in proliferation were observed (Fig. 1, *D* and *E*).

The strong protection from activation-induced cell death following miR-191 overexpression indicates a profound role for miR-191 in T cell survival. Whether miR-191 was essential for T cell development, survival, or function was determined using mice with T cell-intrinsic miR-191 deficiency. A conditional transgenic mouse strain was generated directly on the C57BL/6 background carrying a floxed miR-191 locus (miR-$191^{f/f}$). Our design ensured that the insertion of loxP sites did not interfere

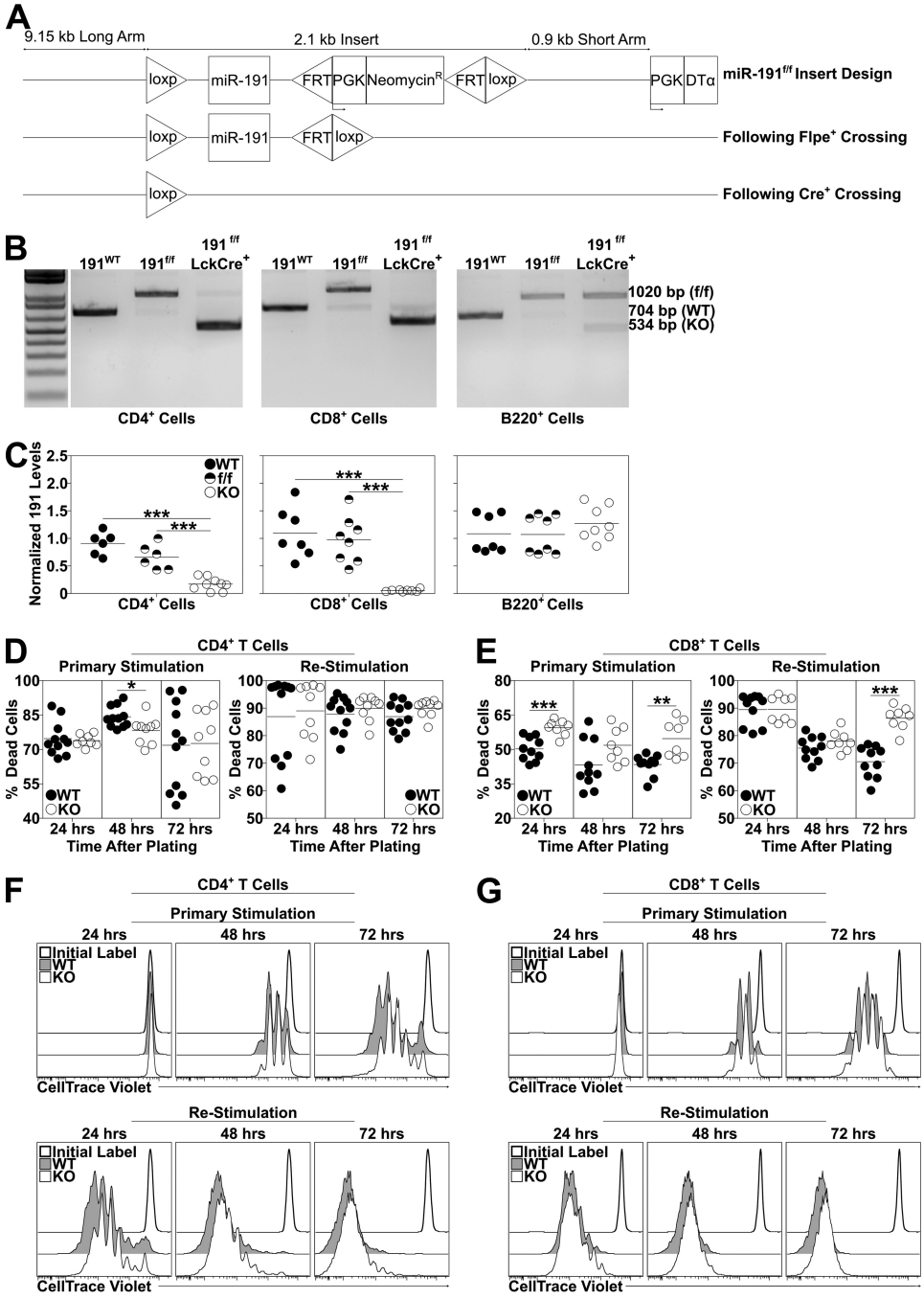

FIGURE 2. **Loss of miR-191 in T cells impairs their survival following stimulation *in vitro*.** *A*, design of the miR-191f/f construct. A loxP site is placed upstream, and a FRT-flanked neo cassette is placed downstream, followed by another loxP site. Following Flpe action, the neo cassette is deleted, but miR-191 is intact. Only Cre recombinase action removes miR-191. *B*, PCR of the miR-191 locus from MACS-purified LN B220$^+$ B cells (*left panel*), CD4$^+$ T cells (*center panel*), and CD8$^+$ T cells (*right panel*) from animals of the indicated genotypes. A ladder is shown with bands ranging from 100–2000 bp. The wild-type miR-191 band is 704 bp, the floxed miR-191 band is 1020 bp, and the knockout band is 534 bp. Data are representative of two independent experiments. *C*, RT-qPCR for miR-191 expression in MACS-purified LN B220$^+$ B cells (*left panel*), CD4$^+$ T cells (*center panel*), and CD8$^+$ T cells (*right panel*) from animals of the indicated genotypes. Expression levels were normalized using geNorm. Data are from two independent experiments ($n = 6$–7/group). *D*–*G*, CD4$^+$ and CD8$^+$ T cells were purified by MACS or FACS, stimulated with plate-bound α-CD3ϵ/CD28 for 24 h, and analyzed at the indicated times post-plating by flow cytometry. *D* and *E*, summary of cell death following primary stimulation (*left panel*) and restimulation (*right panel*). *F* and *G*, representative MFI plots for CellTrace Violet levels in live cells following primary stimulation (*top panel*) and restimulation (*bottom panel*). Data are from three independent experiments ($n = 4$–7/group). Differences in group means were determined by unpaired Student's *t* test: *, $p < 0.05$; **, $p < 0.01$; ***, $p < 0.001$.

with miRNA expression and processing by placing all genetic modifications at least 100 bp away from the pre-miRNA sequence (Fig. 2*A*). Breeding the miR-191$^{f/f}$ mice to mice expressing Cre recombinase under the proximal Lck promoter (LckCre$^+$) resulted in miR-191 deletion specifically in T cells beginning at the DN2 stage of thymocyte development (19). Specific deletion of the miR-191 locus was observed in CD4$^+$ and CD8$^+$ T cells but not B cells (Fig. 2*B*), and concomitant reductions in the miR-191 transcript were observed in CD4$^+$ and CD8$^+$ T cells from LckCre$^+$ mice (Fig. 2*C*). miR-191$^{f/f}$Lck-

Cre^+ mice were viable and fertile and exhibited no gross physical abnormalities. Following stimulation and restimulation through the TCR, $CD8^+$ but not $CD4^+$ T cells lacking miR-191 underwent progressively accelerated cell death over time (18–26%; Fig. 2, *D* and *E*). Similar to miR-191 overexpression, proliferation was unaffected by miR-191 depletion (Fig. 2, *F* and *G*). miR-191 expression therefore promotes T cell survival, and, in its absence, T cells die more rapidly following TCR stimulation.

miR-191 Deficiency Leads to Peripheral T Cell Loss—T cell development and survival *in vivo* was then evaluated in miR-191-deficient mice. T cell-intrinsic miR-191 deficiency in 8-week-old adult mice led to a consistent and significant loss of peripheral $CD4^+$ and $CD8^+$ T cell numbers (30% ± 6% and 49% ± 3%, respectively; Fig. 3*A*). This deficiency did not recover as mice aged, as 30-week-old aged mice had similar reductions in $CD4^+$ and $CD8^+$ T cells (34% ± 8% and 45% ± 11%, respectively; Fig. 3*A*). T_{Regs} were also significantly reduced in number in the absence of miR-191 in young adult and aged mice (42% ± 7% and 49% ± 2%, respectively; Fig. 3*B*). T_{Regs} were modestly reduced by proportion, but this did not alter the homeostatic proportions of naïve ($CD44^-CD62L^+$) or activated ($CD44^+CD62L^-$) $CD4^+$ or $CD8^+$ T cells (Fig. 3, *C* and *D*). Reductions in naïve and memory T cell numbers in these unchallenged animals were proportional to the overall reduction in T cell cellularity. $CD8^+$ and T_{Reg} cell loss was also observed in the spleens of miR-191-deficient mice at 8 but not 30 weeks of age (Fig. 3, *E* and *F*). Homeostatic activation in the spleen was largely unaffected by the loss of miR-191 (Fig. 3, *G* and *H*).

Whether the loss of peripheral T cell numbers was reflective of gross defects in thymic T cell development was evaluated in miR-191-deficient mice. There were no significant alterations to the proportions of thymic T cell subpopulations, but young adult mice showed a consistent reduction in overall thymic cellularity stemming from losses in the $CD4^+CD8^+$ double-positive and CD4 single-positive compartments (29% ± 10% and 23% ± 2%, respectively; Fig. 4*A*). Thymic T_{Reg} frequencies were not altered in the absence of miR-191, although total numbers were marginally reduced at rates proportional to the observed reduction in overall thymic cellularity (Fig. 4*B*). The reduction in $CD4^+CD8^+$ double-positive cell numbers was preceded by modest reductions in the proportion and number of DN2 cells (47% ± 13%, Fig. 4*C*). Thus, in the absence of miR-191, T cell development in the thymus is grossly normal.

miR-191 Deficiency Results in $CD8^+$ T Cell Loss Following Immunization—To determine whether the peripheral loss of $CD4^+$ and $CD8^+$ T cells in naïve mice affects an active immune response, wild-type and miR-$191^{f/f}LckCre^+$ mice were immunized with OT-I ($CD8^+$ T cell-specific) and OT-II ($CD4^+$ T cell-specific) peptides. Following primary immunization, the total number of $CD8^+$ T cells was still reduced in the periphery (51% and 62% reductions in the spleen and lymph nodes, respectively; Fig. 5*A*). T_{Reg} numbers were also reduced in the lymph node (46%, Fig. 5*B*). However, no proportional alterations were observed for activation, as assessed by CD44 *versus* CD62L staining (Fig. 5, *C* and *D*). Further, no differences were observed in the generation of $CD4^+$ effector ($CD162^+Ly6C^+$), prememory ($CD162^+Ly6C^-$), or follicular helper ($CD162^-Ly6C^-$) T cells (20) (Fig. 5*E*). $CD8^+$ effectors ($Ly6C^-$) (21, 22) were proportionately reduced in both the spleen and lymph nodes of miR-$191^{f/f}LckCre^+$ mice (14% and 17%, respectively; Fig. 5*F*). T cell proliferation was then assessed directly *ex vivo* to determine whether the reduction of $CD8^+$ T cell numbers from miR-191-deficient animals resulted from cell death or deficient proliferation. No difference was observed in the incorporation of EdU (Fig. 5*G*). Finally, T cells from immunized mice were restimulated with OT-I or OT-II peptides to determine whether the observed cell loss was due to antigen-specific stimulation. $CD8^+$ T cells from both the spleen and lymph nodes showed impaired survival after 5 h of stimulation (19% and 13%, respectively; Fig. 5*H*). As OT-I and OT-II-specific precursors are quite limited in individual mice, this reduction indicates a potentially significant difference in antigen-specific responses in the absence of miR-191. Thus, miR-191 controls the homeostatic maintenance of T cells and further supports cell survival during an effector response.

miR-191 Enables Cytokine-driven Homeostatic Survival—Peripheral T cell maintenance relies on tonic TCR signaling and appropriate cytokine signaling, and diminished signaling reduces cell survival in peripheral lymphoid tissues. To address whether peripheral T cell loss resulted from insufficient cytokine-driven homeostatic maintenance, naïve ($CD44^-CD62L^+$) and central memory ($CD44^+CD62L^+$) $CD8^+$ T cells and T_{Regs} were isolated and cultured *in vitro* with the appropriate homeostatic cytokines required for the survival of these subsets (IL-7, IL-15, and TCR plus IL-2, respectively). For each of these populations, the loss of miR-191 resulted in increased cell death (21%-70%; Fig. 6, *A*–*C*).

As the IL-2, IL-7, and IL-15 receptors require CD132, CD132 expression was evaluated among $CD4^+$ and $CD8^+$ T cells directly *ex vivo*. CD132 levels were equivalent among $CD4^+$ and $CD8^+$ T cells with and without miR-191 (Fig. 6*D*). Downstream of CD132, the IL-2, IL-7, and IL-15 signaling pathways converge at the activation of the transcription factor STAT5. Tyrosine 694 phosphorylation is critical to activate STAT5 and initiate transcriptional programs for STAT5-dependent homeostatic survival, particularly for $CD8^+$ T cells and T_{Regs} (23, 24). Although STAT5 protein levels are equivalent regardless of the presence of miR-191 (Fig. 6*E*), both early and peak phosphorylation of STAT5 on Tyr^{694} is significantly reduced in $CD8^+$ cells lacking miR-191 (20%-40% reductions, Fig. 6*F*). miR-191 therefore facilitates homeostatic survival following cytokine signaling that relies on STAT5 tyrosine phosphorylation.

miR-191 Targets the Scaffolding Molecule Irs1—The impaired phosphorylation response downstream of cytokine signaling did not result from deficiencies in total STAT5 or CD132, suggesting that miR-191 specifically regulates a different gene or gene set related to this pathway. Phenotypically relevant targets of miR-191 were predicted computationally using the TargetScan algorithm (25). Humans and mice share 86 predicted targets for miR-191 (supplemental Table 1). RT-qPCR screening for these targets in $CD4^+$ T cells from wild-type and miR-$191^{f/f}LckCre^+$ animals yielded a single gene consistently detectable in T cells and with elevated expression in cells lacking miR-191: insulin receptor substrate 1 (*Irs1*). In both human and mouse, the 3′ UTR of (mRNA) *IRS1* contains

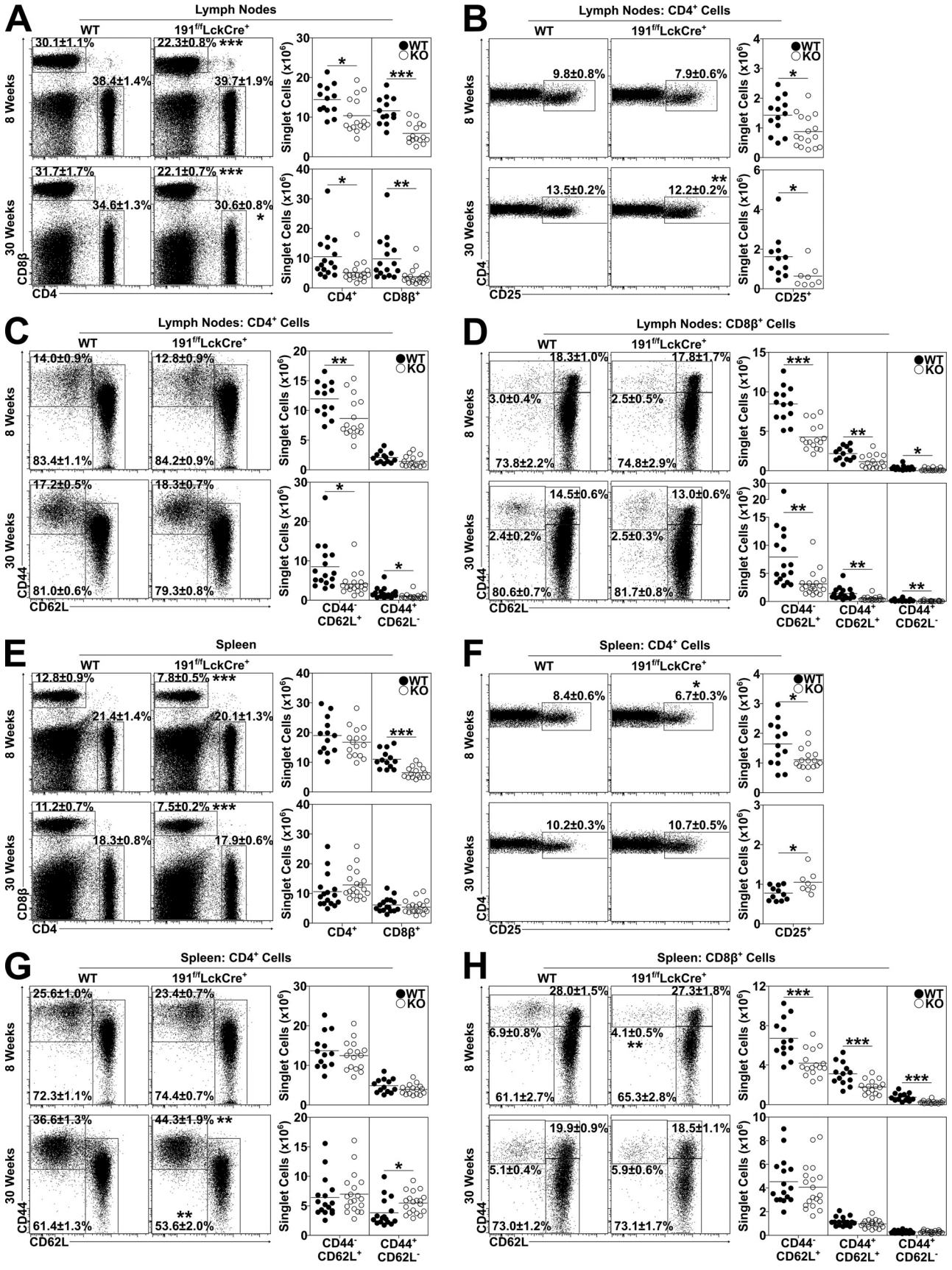
A
Lymph Nodes
WT
191f/fLckCre+
8 Weeks
30 Weeks
CD8β
CD4
30.1±1.1%
22.3±0.8% ***
38.4±1.4%
39.7±1.9%
31.7±1.7%
22.1±0.7% ***
34.6±1.3%
30.6±0.8%
*
Singlet Cells (x10^6)
WT
KO
CD4+
CD8β+
B
Lymph Nodes: CD4+ Cells
9.8±0.8%
7.9±0.6%
13.5±0.2%
12.2±0.2%
**
CD25
CD25+
C
Lymph Nodes: CD4+ Cells
CD44
CD62L
14.0±0.9%
12.8±0.9%
83.4±1.1%
84.2±0.9%
17.2±0.5%
18.3±0.7%
81.0±0.6%
79.3±0.8%
CD44- CD62L+
CD44+ CD62L-
D
Lymph Nodes: CD8β+ Cells
18.3±1.0%
17.8±1.7%
3.0±0.4%
2.5±0.5%
73.8±2.2%
74.8±2.9%
14.5±0.6%
13.0±0.6%
2.4±0.2%
2.5±0.3%
80.6±0.7%
81.7±0.8%
CD44+ CD62L+
E
Spleen
12.8±0.9%
7.8±0.5% ***
21.4±1.4%
20.1±1.3%
11.2±0.7%
7.5±0.2% ***
18.3±0.8%
17.9±0.6%
F
Spleen: CD4+ Cells
8.4±0.6%
*
6.7±0.3%
10.2±0.3%
10.7±0.5%
G
Spleen: CD4+ Cells
25.6±1.0%
23.4±0.7%
72.3±1.1%
74.4±0.7%
36.6±1.3%
44.3±1.9% **
61.4±1.3%
**
53.6±2.0%
H
Spleen: CD8β+ Cells
28.0±1.5%
27.3±1.8%
6.9±0.8%
4.1±0.5%
**
61.1±2.7%
65.3±2.8%
19.9±0.9%
18.5±1.1%
5.1±0.4%
5.9±0.6%
73.0±1.2%
73.1±1.7%

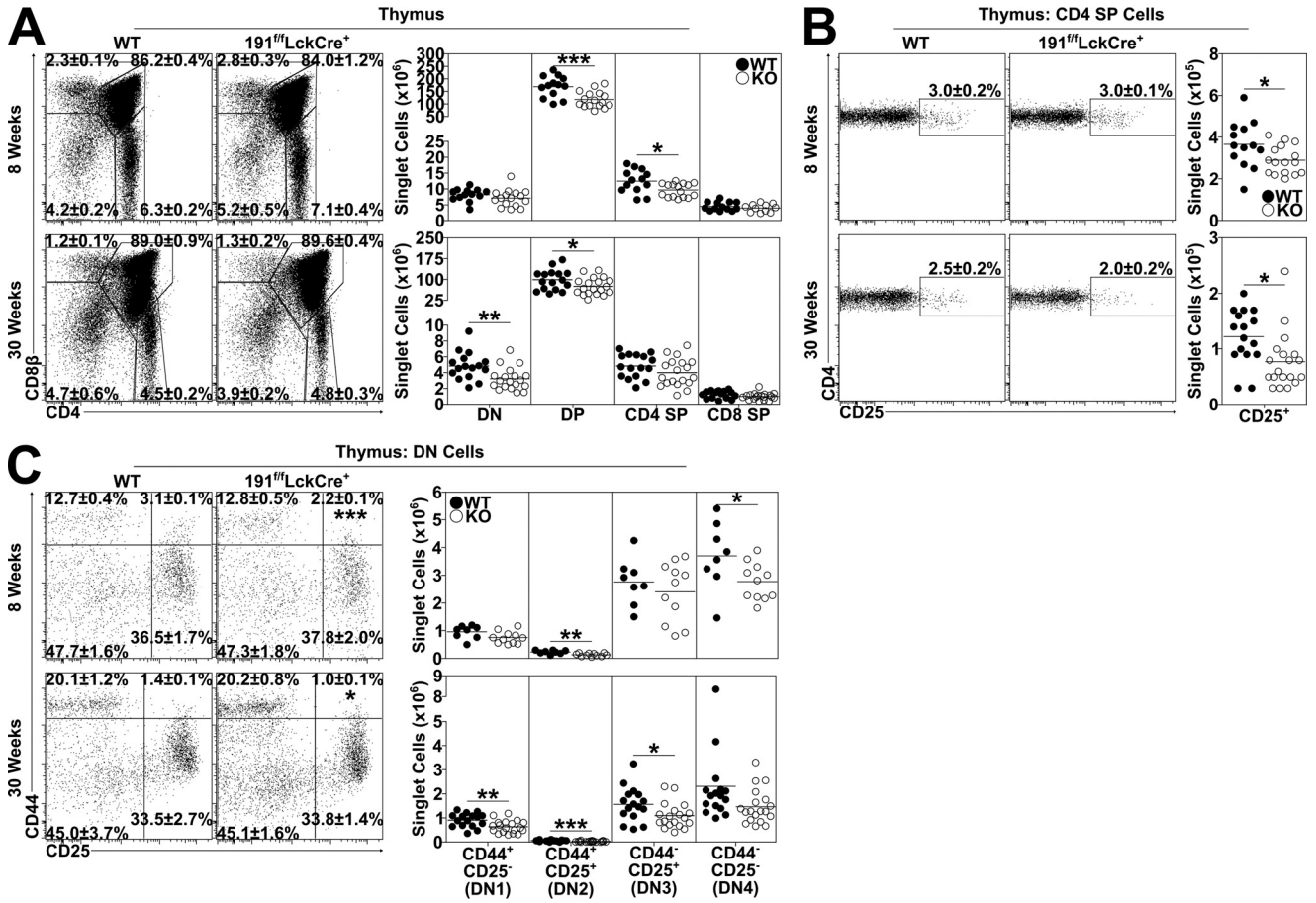

FIGURE 4. **Loss of miR-191 during DN2 modestly impacts T cell development.** All panels show representative dot plots (*left panels*) and a summary of cell numbers for the specified populations (*right panels*) from 8-week-old (*top panels*) and 30-week-old (*bottom panels*) animals. The populations examined were thymocytes (*A*), regulatory T cells in the thymus (*B*), and double-negative thymocytes (*C*). Data are from four independent experiments ($n = 8–19$/group. Differences in group means were determined by unpaired Student's *t* test: *, $p < 0.05$; **, $p < 0.01$; ***, $p < 0.001$.

one miR-191 target site (Fig. 7*A*), although the 3′ UTR of (mRNA) *IRS1* is not highly conserved. Similarly, other species, including *Canis lupus familiaris*, *Bos taurus*, and *Rattus norvegicus*, contain miR-191 target sites in the 3′ UTR of (mRNA) *Irs1* (data not shown), suggesting functional conservation of miR-191 targeting (mRNA) *Irs1*. IRS1 is a scaffolding protein that brings p85 and Grb2 to the insulin receptor (26, 27). IRS1 in human T cells co-precipitates with both JAK1 and JAK3, and this association is enriched during the course of cytokine signaling downstream of CD132 (28). To demonstrate directly that miR-191 can bind to the 3′ UTR of (mRNA) *Irs1* and block protein synthesis, a 3′ UTR luciferase assay was performed. Overexpression of miR-191 resulted in down-regulation of firefly luciferase activity (21%, Fig. 7*B*) when the full-length 3′ UTR of (mRNA) *Irs1* was cloned downstream; luciferase activity was restored with mutation of the miR-191 target site. These data show that miR-191 targets (mRNA) *Irs1* directly. To determine whether miR-191 targets (mRNA) *Irs1* in murine T cells, *Irs1* transcript and intracellular IRS1 protein levels were measured. $CD8^+$ T cells lacking miR-191 showed a modest up-regulation in *Irs1* transcript levels (Fig. 7*C*), whereas both $CD4^+$ and $CD8\beta^+$ T cells lacking miR-191 had increased IRS1 protein (24% and 38%, $p < 0.01$ and $p < 0.05$, respectively; Fig. 7*D*). To directly determine whether elevated IRS1 levels enhance T cell death, wild-type $CD8^+$ T cells were retrovirally induced to overexpress IRS1. $CD8^+$ T cells were then cultured in serum-free medium containing IL-2 to determine the rate of cytokine-induced survival. Cells overexpressing IRS1 (62% increase in IRS1 levels, Fig. 7*E*) showed a concomitant 67% decrease in survival relative to cells expressing the mock vector (Fig. 7*F*). miR-191 therefore targets (mRNA) *Irs1*, and increased IRS1 levels induce cell death following stimulation.

Discussion

This study uncovered a miRNA, miR-191, that plays a profound role in the homeostatic maintenance of the adaptive immune system. miR-191 was shown to support cytokine-dependent naïve, memory, and regulatory T cell survival at home-

FIGURE 3. **miR-191 supports peripheral T cell survival at homeostasis.** All panels show representative dot plots (*left panels*) and a summary of cell numbers for the specified populations (*right panels*) from 8-week-old (*top panels*) and 30-week-old (*bottom panels*) animals. The populations examined were peripheral lymphocytes (*A*), peripheral regulatory T cells (*B*), peripheral $CD4^+$ T cells (*C*), peripheral $CD8^+$ T cells (*D*), splenocytes (*E*), splenic regulatory T cells (*F*), splenic $CD4^+$ T cells (*G*), and splenic $CD8^+$ T cells (*H*). Data are from two to four independent experiments ($n = 8–19$/group). Differences in group means were determined by unpaired Student's *t* test: *, $p < 0.05$; **, $p < 0.01$; ***, $p < 0.001$.

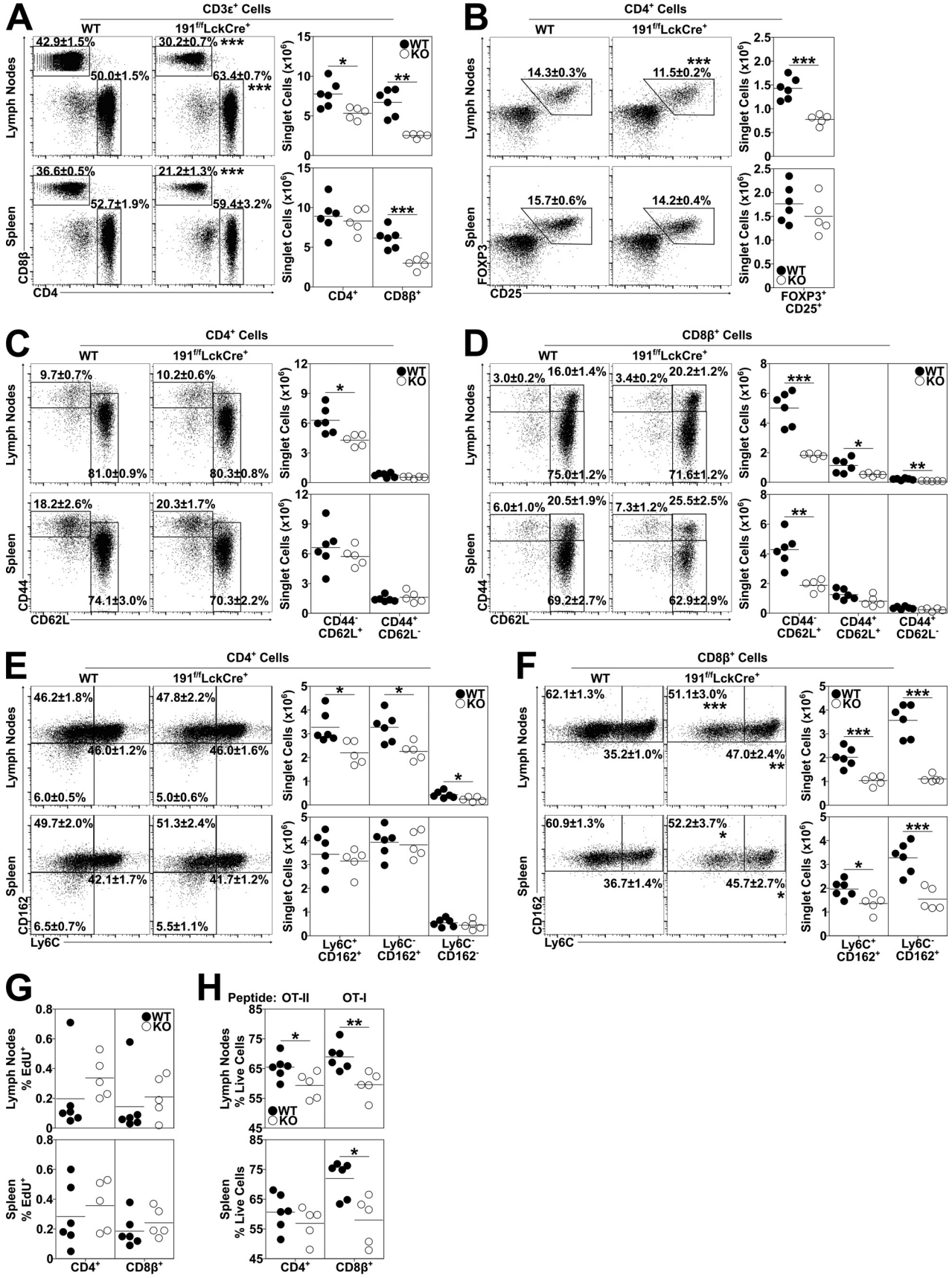
A
CD3ε+ Cells
WT
191f/fLckCre+
Lymph Nodes
Spleen
CD8β
CD4
42.9±1.5%
50.0±1.5%
30.2±0.7%
63.4±0.7%
36.6±0.5%
52.7±1.9%
21.2±1.3%
59.4±3.2%
Singlet Cells (x10^6)
WT
KO
CD4+
CD8β+
B
CD4+ Cells
14.3±0.3%
11.5±0.2%
15.7±0.6%
14.2±0.4%
FOXP3
CD25
FOXP3+ CD25+
C
CD4+ Cells
9.7±0.7%
10.2±0.6%
81.0±0.9%
80.3±0.8%
18.2±2.6%
20.3±1.7%
74.1±3.0%
70.3±2.2%
CD44
CD62L
CD44- CD62L+
CD44+ CD62L-
D
CD8β+ Cells
3.0±0.2%
16.0±1.4%
3.4±0.2%
20.2±1.2%
75.0±1.2%
71.6±1.2%
6.0±1.0%
20.5±1.9%
7.3±1.2%
25.5±2.5%
69.2±2.7%
62.9±2.9%
E
CD4+ Cells
46.2±1.8%
47.8±2.2%
46.0±1.2%
46.0±1.6%
6.0±0.5%
5.0±0.6%
49.7±2.0%
51.3±2.4%
42.1±1.7%
41.7±1.2%
6.5±0.7%
5.5±1.1%
CD162
Ly6C
Ly6C+ CD162+
Ly6C- CD162+
Ly6C- CD162-
F
CD8β+ Cells
62.1±1.3%
51.1±3.0%
35.2±1.0%
47.0±2.4%
60.9±1.3%
52.2±3.7%
36.7±1.4%
45.7±2.7%
G
Lymph Nodes % EdU+
Spleen % EdU+
CD4+
CD8β+
H
Peptide: OT-II
OT-I
Lymph Nodes % Live Cells
Spleen % Live Cells

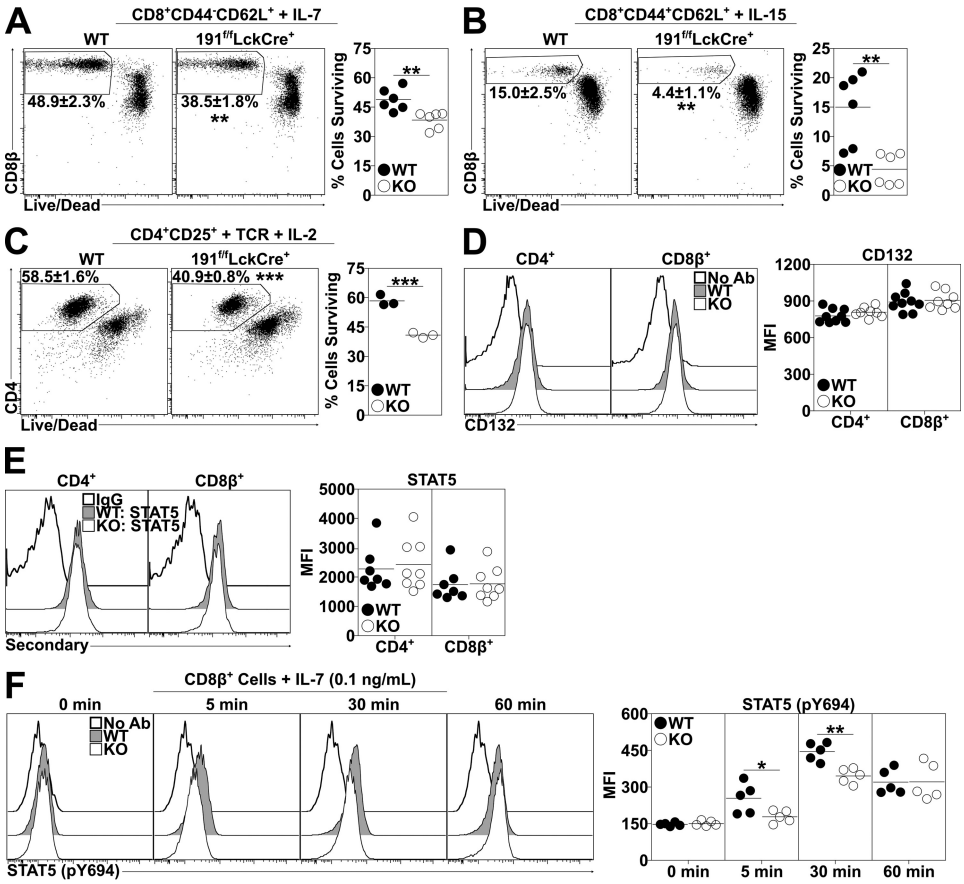

FIGURE 6. **miR-191 promotes homeostatic STAT5-dependent cytokine signaling.** *A–C*, sorted CD44$^-$CD62L$^+$ (*A*) and CD44$^+$CD62L$^+$ (*B*) CD8$^+$ cells and CD4$^+$CD25$^+$(*C*) cells were cultured *in vitro* with the homeostatic cytokines most important for the survival of these subsets (IL-7, IL-15, and TCR plus IL-2, respectively). Representative dot plots (*left panels*) and summary plots (*right panels*) are shown. Data are from one to two independent experiments (n = 3–6/group). *D* and *E*, representative MFI plots (*left panels*) and summary plots (*right panels*) for CD132 (*D*) and STAT5 (*E*) staining in splenic CD4$^+$ and CD8β^+ cells. Data are from two independent experiments (n = 7–9/group). *F*, MACS-isolated CD8$^+$ T cells were stimulated *ex vivo* with IL-7, and pSTAT5 levels were assessed via flow cytometry at the indicated time points. Representative MFI plots (*left panel*) and summary data (*right panel*) are shown. Data are from two independent experiments (n = 5/group). Differences in group means were determined by unpaired Student's t test: *, $p < 0.05$; **, $p < 0.01$; ***, $p < 0.001$.

ostasis by controlling the levels of IRS1 and thereby the activation kinetics of STAT5. IRS1 was initially described as the principal substrate for signal transduction downstream of the insulin receptor (29). Signaling through the insulin receptor phosphorylates critical tyrosines on IRS1, resulting in the recruitment and activation of various SH2 domain-containing proteins, including the p85 subunit of PI3K (26) and GRB2 (27). Early studies in human T cells found that IRS1 associates with JAK1 and JAK3 in the absence of cytokine and that the addition of IL-2 or IL-4 increases this association (28). Further, these same studies revealed that cytokine signaling induces p85 PI3K association with IRS1. Later experiments demonstrated that IL-7 signaling in human thymocytes drives increased association between IRS1 and JAK1, JAK3, and p85 (30). These data support a model in which IRS1 positions at the cytokine receptor by interacting with JAK1 and JAK3. Following cytokine signaling, IRS1 activates p85 and GRB2, driving both PI3K and MAPK signaling. PI3K-mediated mechanistic target of rapamycin (mTOR) activation results in hyperphosphorylation of N-terminal serine residues on IRS1. This hyperphosphorylation then leads to IRS1 associating with FBW8 (part of the cullin RING E3 ubiquitin ligase 7 complex), resulting in poly-ubiquitination and proteasomal degradation (31).

In normal T cells, there is a balance between the amount of IRS1 bound to JAK1 and JAK3 and the amount of JAK1 and JAK3 free to phosphorylate STAT5. However, in the absence of miR-191, increased IRS1 protein may result in excessive interaction between IRS1 and JAK1 and JAK3. This could sequester the two kinases from the common γ chain receptor, resulting in deficient STAT5 activation. Indeed, we observed deficient STAT5 phosphorylation in cells lacking miR-191 as well as diminished naïve, regulatory, and memory cell numbers. STAT5 is an important regulator of survival downstream of cytokine signaling. Mice lacking the entire *Stat5* locus (STAT5-

FIGURE 5. **Loss of miR-191 results in reduced CD8$^+$ T cell numbers during immunization.** All panels provide data from both lymph nodes (*top panels*) and spleen (*bottom panels*) and are from two independent experiments (n = 5–6/group). *A–F*, direct *ex vivo* staining with representative dot plots (*left panels*) and a summary of cell numbers for the specified populations (*right panels*). The populations examined were CD3ϵ^+ cells (*A*), peripheral regulatory T cells (*B*), peripheral CD4$^+$ T cells (*C* and *E*), and peripheral CD8$^+$ T cells (*D* and *F*). *G*, proportion of cells staining positive for EdU after 2 h of labeling *ex vivo*. *H*, proportion of cells surviving after 5 h of *ex vivo* stimulation with OT-I or OT-II peptide. Differences in group means were determined by unpaired Student's t test: *, $p < 0.05$; **, $p < 0.01$; ***, $p < 0.001$.

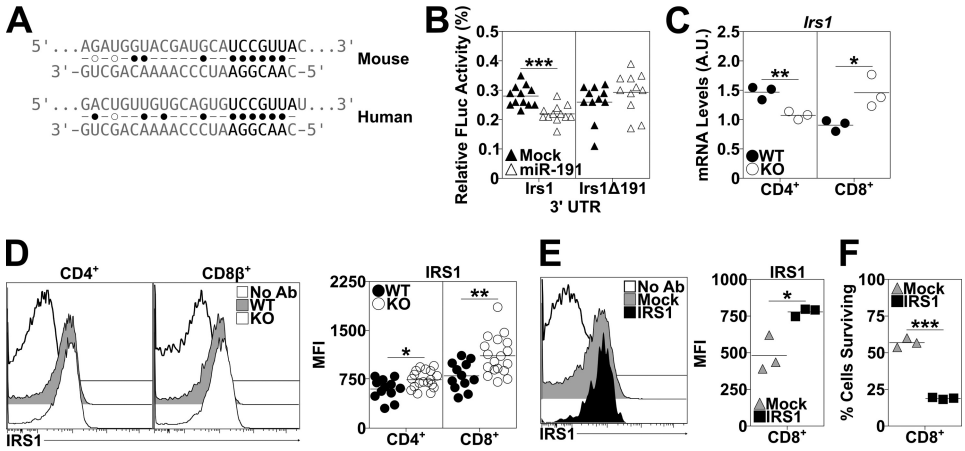

FIGURE 7. **miR-191 targets Irs1.** *A*, alignment of miR-191 (*bottom strand*) with its target site in the 3′UTR of the *Irs1* transcript (*top strand*) for both mice and humans. *B*, firefly luciferase activity in NIH-3T3 cells transfected with mock-GFP or miR-191-GFP plasmids with pmiRGLO containing either wild-type or miR-191 target site deleted versions of the *Irs1* 3′ UTR downstream of firefly luciferase. Data were normalized to internal *Renilla* luciferase expression. Data are from three independent experiments ($n = 11$–12/group). *C*, RT-qPCR for *Irs1* transcript expression in MACS-purified splenic $CD4^+$ and $CD8^+$ cells. Expression levels were normalized using geNorm. Data are from a single experiment. *D*, IRS1 staining by flow cytometry in splenic $CD4^+$ and $CD8\beta^+$ cells. Representative MFI plots (*left panel*) and summary data (*right panel*) are shown. Data are from three independent experiments ($n = 12$–18/group. *E* and *F*, $CD8^+$ T cells were purified by MACS, infected with mock-GFP or pBABE-IRS1 retrovirus, puromycin-selected, restimulated with IL-2 for 24 h, and then analyzed for IRS1 expression (*E*) and survival (*F*) by flow cytometry. Data are from a single experiment ($n = 3$/group). Differences in group means were determined by unpaired Student's *t* test: *, $p < 0.05$; **, $p < 0.01$; ***, $p < 0.001$.

deficient) exhibit almost complete perinatal lethality, with the rare surviving mice exhibiting SCID-type symptoms and a near absence of thymocytes, in addition to dramatic reductions in T, B, and natural killer cells in the periphery (32). In this study, we observed proportionately normal thymic development but a 30% decrease in thymic cellularity and 40%-50% losses in regulatory and $CD8^+$ T cells in the peripheral lymph nodes. Our data very closely resemble early studies of STAT5-deficient mice in which the targeting strategy actually resulted in N-terminally truncated but partially functional STAT5 ($STAT5^{\Delta N}$ (23, 33)). $STAT5^{\Delta N}$ mice show grossly normal thymic development but exhibit 50% reductions in thymocyte numbers (34) and have preferential loss of $CD8^+$ and regulatory T cells in the periphery (23, 24). Similarly, the inhibition of STAT5 tetramer formation leads to preferential loss of $CD8^+$ T cells in the periphery and fewer functional regulatory cells (35). Thus, modest perturbations in STAT5 signaling lead to significant defects in T cell survival, and miR-191 regulation of IRS1 downstream of cytokine signaling is a key rheostat of homeostatic STAT5 signaling.

In the last decade, many studies have collectively demonstrated that miRNAs are significant regulators of many distinct molecular networks. However, only a handful of studies have observed a role for miRNAs in regulating immune system homeostasis. These studies report either dramatic alterations in lymphocyte development that then lead to peripheral defects (36) or involve the use of global knockouts and see multiple confounding disruptions (37–39). Our study evaluated the specific role miR-191 plays in T cell development and function using a conditional deletion system. Although this system deleted miR-191 in thymocytes during the late DN2 stage of development, no gross abnormalities in thymic T cell development were observed. Rather, these data revealed a novel role for miRNAs in the physiologic maintenance of T cells in the periphery in a mechanism dependent on fine-tuning intracellular cytokine signaling. Such fine manipulation is likely part of a much larger network of genetic and epigenetic regulators that guide lymphocyte fate decisions at homeostasis.

Just as perturbations within the regulatory network affect T cell phenotypes, altered T cell homeostasis likely impacts other cells. As an example, it is known that dendritic cells (DCs) act as a critical source of IL-7 for $CD4^+$ T cells but not $CD8^+$ T cells, which receive IL-7 from the stroma of lymphoid tissues. When IL-7 levels increase, such as when there is a sharp reduction in peripheral T cell numbers, DCs down-regulate IL-7 production as well as MHC II expression, events that then impair the survival of $CD4^+$ T cells at homeostasis (40). Thus, further investigation is needed to determine whether the loss of $CD4^+$ T cells in miR-$191^{f/f}$$LckCre^+$ animals arises strictly from a cell-intrinsic defect in the response to homeostatic cytokines or whether $CD8^+$ T cell loss results in enhanced IL-7 and DC deficiencies that also contribute to diminished $CD4^+$ T cell survival. Altered DC homeostasis would also likely impact T cell priming during immune responses and is therefore an important area for future investigation.

Cytokine signaling is also crucial to productive ongoing immune responses, and although previous work showed STAT5 to be largely dispensable for $CD8^+$ T cell effector function during a primary immune response (41–43), IRS1 was recently shown to negatively regulate STAT3 activation (44) and so likely impacts other STATs in T cells, potentially altering memory formation and/or differentiation. Future studies to address these issues may wish to apply TCR repertoire analysis or TCR transgenics and cell transfer to meaningfully investigate the role of miR-191 and IRS1 in T cell effector responses. Future studies will also need to address the role of miR-191 in B cells, as they also show consistently high expression of miR-191 (data not shown and Ref. 18). Such work will also need to investigate whether miR-191 has alternate or additional targets in other cell types, as different mRNA and miRNA pools may shift phenotypically relevant miR-191 targeting. Importantly, we demonstrated that the manipulation of miR-191 alters T cell

homeostasis without leading to severe immunodeficiency or autoimmunity. As much data exists on the causative agents disrupting active immune responses and the formation of immunological memory, we must also understand the basic processes underlying the continued maintenance of a functioning immune system so that we might promote healthy immune function throughout the life of the individual.

Experimental Procedures

Mice—Mice designated "wild-type" were C57BL/6 mice expressing CD90.1 and CD45.1 (B6.PL-*Thy1*^{a}/CyJ crossed with B6.SJL-*Ptprc*^{a} *Pepc*^{a}/BoyJ) from The Jackson Laboratory (Bar Harbor, ME).

The floxed miR-191 (miR-191$^{f/f}$) construct was generated by PCR amplification of a 9.15-kb long arm, 900-bp short arm, and the pre-miR-191 sequence with at least 100-bp flanking sequence from bacterial artificial chromosome clone RP23–225E15 (CHORI BACPAC, Oakland, CA) using high-fidelity Velocity polymerase (Bioline, Taunton, MA) and the following primers from IDT (Coralville, IA): 5′-AGT TCC GCG GCG GCT TAA TTA AGG TTA TTG GCC TTT GCT GCT-3′/5′-ATG ACC TGT AGA CTG GGA TAC TTC TC CTT GAT GT-3′ (5′ half of long arm), 5′-CCT GTT CTA GGA CTC TTC CCA GGG AAA CTC-3′/5′-ACA AGC GGC CGC AAA CCA GTC TAG TGA GAA TGA GAC G-3′ (3′ half of long arm), 5′-TCA AGT CGA CGG TGG CAG TCA GAG GCG ACG AAA AAA G-3′/5′-AGT TGA TAT CCT GCC TCT GCC TCC TGA GTA-3′ (short arm), and 5′-AAT ACC CGG GAA AAC ACC TAC TCC TTC CTA CTC AGC CCA-3′/5′-GTT ACA ATT GAT CAG TCT GGG GGT GCA CCT GAG AGA TGG-3′. Fragments were cloned into a targeting vector using the following cut sites: SacII-BclI and BclI-NotI for the 5′ and 3′ long arm sides, respectively; SalI-EcoRV for the short arm; and XmaI-MfeI for miR-191. The targeting vector was linearized with PacI, and the targeting fragment was purified following agarose gel electrophoresis and then introduced into C57BL/6N-PRX-B6N #1 embryonic stem cells (ESCs) (The Jackson Laboratory). Positive ESC clones were detected by PCR using the following primers: 5′-CGC CTT CTT GAC GAG TTC TTC TG-3′/5′-TTT CCT GTA TTC ATG AGC CCT AAC C-3′. Chimeric mice were generated by microinjecting appropriately targeted ESC clones into C57BL/6 blastocysts at the Duke Transgenic Mouse Shared Resource (Duke University, Durham, NC). A single clone produced viable pups, and correct integration of the targeting construct was confirmed by PCR-amplifying a 10.98-kb fragment containing floxed miR-191 and extending into the genome using Ranger Polymerase (Bioline) and the following primers: 5′-GAG TGA TAA TGT CTG GTG TGC CCT G-3′/5′-TTG TGT AGC GCC AAG TGC CC-3′. Mice containing floxed miR-191 were crossed to Flpe (C57BL/6-Tg(CAG-Flpe)2Arte) mice from Taconic Farms (Hudson, NY) to eliminate the PGKneo cassette and were then backcrossed to wild-type mice to eliminate the Flpe transgene and produce miR-191$^{f/f}$ mice. miR-191$^{f/f}$ mice were crossed to Lck-Cre (B6.Cg-Tg(lck-cre)1Cwi N9) mice from Taconic Farms to delete miR-191 specifically in T cells. All mice were housed under specific pathogen-free conditions. All studies were approved by the Institutional Animal Care and Use Committee at Duke University.

Cell Preparation and Immunofluorescence Analysis—Single-cell leukocyte suspensions from thymus, spleen, and peripheral lymph nodes (superficial cervical, axillary, brachial, inguinal, and mesenteric) were generated by gentle dissection, and erythrocytes were hypotonically lysed using ammonium-chloride-potassium lysing buffer. For multicolor immunofluorescence analysis of surface proteins, viable single-cell suspensions (1×10^6) in PBS were blocked for 10 min on ice with 0.8 μg of anti-CD16/CD32 (2.4G2) from Bio X Cell (West Lebanon, NH) in 100 μl. Cells were then stained for 15 min at room temperature using predetermined optimal concentrations of mAb in FACS buffer (DPBS (pH 7.4), 2 mM EDTA, and 2% FCS). For analysis of intracellular proteins, cells were then washed with DPBS and fixed in DPBS containing 2% paraformaldehyde for 10 min at room temperature. Cells were washed with FACS buffer and then resuspended in FACS buffer with 0.1% saponin (Sigma-Aldrich, St. Louis, MO), held at room temperature for 10 min, and then stained with predetermined optimal concentrations of antibodies. Samples requiring methanol permeabilization (STAT5 and STAT5-Tyr(P)^{694}) were first fixed with 2% paraformaldehyde for 10 min at room temperature, washed in FACS buffer, resuspended in 10% 1× DPBS/90% ice-cold methanol, held at 4 °C for 10 min, and then either stored at −20 °C for 24 h or washed with FACS buffer and stained with predetermined optimal concentrations of antibodies in FACS buffer for 30 min at room temperature. If a secondary antibody was needed, cells were washed with FACS buffer and then stained with fluorophore-conjugated secondary for 15 min at room temperature. For samples requiring staining of FOXP3, the FOXP3/transcription factor staining buffer set from eBioscience (San Diego, CA) was used according to the instructions of the manufacturer. After staining and a final FACS buffer wash, cells were resuspended in FACS buffer containing 0.5% paraformaldehyde and kept in the dark at 4 °C until analysis.

Unconjugated antibodies for staining included STAT5 (3H7) from Cell Signaling Technology (Danvers, MA). Pacific Blue-, FITC-, AF-488, phycoerythrin-, PerCp-Cy5.5-, phycoerythrin-Cy7-, allophycocyanin-, AF-647-, and allophycocyanin-Cy7-conjugated antibodies for staining were as follows: CD3ϵ (145–2C11), CD4 (RM4–5), CD8β (YTS156.7.7), CD19 (6D5), CD25 (PC61), CD44 (IM7), L-selectin (CD62L; MEL-14), CD132 (TUGm2), and Ly6C (HK1.4) from BioLegend (San Diego, CA); FOXP3 (FKJ-16S) from eBioscience; CD162 (2PH1) and STAT5-pY694 (47) from BD Biosciences; IRS1 (E-12) from Santa Cruz Biotechnology (Santa Cruz, CA); rabbit IgG from Jackson ImmunoResearch (West Grove, PA); and goat anti-Rabbit IgG from Thermo Fisher Scientific (Waltham, MA).

Cell proliferation was assessed *in vitro* using CellTrace Violet (Thermo Fisher Scientific). Cells were stained with a predetermined optimum concentration of 5 μM according to the instructions of the manufacturer. Proliferation was assessed directly *ex vivo* using the Click-iT Plus EdU flow cytometry assay kit (Thermo Fisher Scientific). Cells (1×10^6) were pulsed with 10 μM EdU for 2 h and then stained according to the instructions of the manufacturer.

Dead cells were identified and excluded from further analysis by staining with Annexin V and 7-Aminoactinomycin D (BioLegend) staining or by staining with the LIVE/DEAD fixable dead cell stain kit (Thermo Fisher Scientific). Single cells with the forward and side light scatter properties of lymphocytes were analyzed using a FACSCanto II flow cytometer (BD Biosciences). Background staining was assessed using isotype-matched controls or a fluorescence minus one control. Data were analyzed using FlowJo v8.2 (FlowJo LLC, Ashland, OR).

Retroviral Infection—Wild-type T cells overexpressing GFP or miR-191-GFP were generated by transfection with an ecotropic retrovirus containing the murine stem cell virus vector (45) with a puromycin-IRES-GFP cassette (46). Pri-miR-191 was amplified from primary splenic T cells and introduced downstream of the 5′ long terminal repeat sequence using XhoI and EcoRI restriction sites. pBABE-puro-mouse-IRS-1-myc (pBABE-IRS1) was a gift from Ronald Kahn (Addgene plasmid 11374) (47).

Plat-E cells (48) grown in complete DMEM (10% NCS, 100 units/ml penicillin, 100 units/ml streptomycin, 2 mM L-glutamine, 1 mM sodium pyruvate, and 0.1 mM nonessential amino acids) supplemented with blasticidin (10 μg/ml) and puromycin (1 μg/ml) were then transduced with the relevant plasmid using Lipofectamine 2000 (Thermo Fisher Scientific), and virus was collected 2 days later for retroviral infection of T cells. T cells were retrovirally infected after 24 h of plate-bound or 2.5 μg/ml concanavalin A (Sigma-Aldrich) stimulation by spinning at 800 $\times$ *g* in a centrifuge maintained at 32 °C for 90 min with 10 μg/ml Polybrene (Sigma-Aldrich).

Plate-bound and Cytokine Stimulation—Plates were prepared by coating the wells of a hydrophilic tissue culture plate with biotinylated poly-L-lysine in DPBS prepared by mixing poly-L-lysine hydrobromide (Sigma-Aldrich) with EZ-link Sulfo NHS-Biotin (Thermo Fisher Scientific). Wells were incubated at room temperature for 1 h with orbital shaking and then washed with DPBS. Wells were then coated with a solution of 1% BSA (Sigma-Aldrich) in DPBS plus 5 μg/ml streptavidin (Prozyme, Hayward, CA), incubated as before, and then washed with DPBS. Wells were then coated with biotinylated mAbs that were prepared by mixing functional-grade anti-CD3ϵ (145–2C11, 1 μg/ml) and anti-CD28 (37.51, 0.2 μg/ml) from Bio X Cell with EZ-link Sulfo NHS-Biotin (Thermo Fisher Scientific) according to the instructions of the manufacturer. Wells were coated with a solution of 1% BSA in DPBS plus biotinylated mAbs either for 1 h at room temperature with orbital shaking or, after 10 min of shaking, placed at 4 °C overnight. Wells were washed again with DPBS before plating cells.

$CD4^+$ or $CD8^+$ T cells were purified by FACS at the Duke Flow Cytometry Shared Resource (Duke University Medical Center) or by MACS using Untouched Mouse CD4 and CD8 kits (Thermo Fisher Scientific) according to the instructions of the manufacturer. T cells were plated at 2 $\times$ 10^6 cells/ml in warm complete RPMI 1640 medium (10% FCS, 50 μM 2-mercaptothanol, 100 units/ml penicillin, 100 units/ml streptomycin, 2 mM L-glutamine, 1 mM sodium pyruvate, and 0.1 mM nonessential amino acids) on coated plates and incubated in a humidified 37 °C incubator with 7% CO_2. For primary stimulation, T cells were given hIL-2 (Peprotech, Rocky Hill, NJ) at 5 ng/ml at plating and 1 ng/ml at each splitting for the first 72 h. Cells receiving puromycin selection were given 3 μg/ml puromycin (Sigma-Aldrich) 24 h after infection, and selection then proceeded for 48 h. Cultures were supplemented with warm, fresh complete RPMI medium as needed. For all restimulations, live cells were isolated using Ficoll-Paque PLUS (GE Healthcare). For α-CD3ϵ/CD28 restimulation, cells were plated at 7.5 $\times$ 10^5 cells/ml in warm complete RPMI on coated plates. For IL-2 restimulation, cells were plated at 5 $\times$ 10^5 cells/ml in U-bottom plates with 5 ng/ml IL-2 in warm, serum-free RPMI with 0.1% BSA.

RT Quantitative PCR (RT-qPCR)—$CD4^+$ and $CD8^+$ T cells and $B220^+$ B cells were purified by MACS (Thermo Fisher Scientific). Cells were washed with DPBS and lysed and homogenized in TRIzol (Thermo Fisher Scientific). Total RNA was extracted using Direct-zol (Zymo Research, Irvine, CA). cDNA was generated using the Flex cDNA synthesis kit (Quanta BioSciences Gaithersburg, MD) with the included oligo(dT) and random primer sets used for mRNA target analysis. For miRNA targets, a poly(A) tail was added using *Escherichia coli* poly(A) polymerase (Epicenter, Madison, WI), and cDNA was then generated using a custom universal tag coupled to oligo(dT) (supplemental Table 1). After first-strand cDNA synthesis, cDNA was diluted in Tricine-EDTA for long-term storage. The qPCR reaction used SYBR Perfecta Supermix (Quanta Biosciences) and unique forward and reverse primers for mRNA targets or a unique forward primer and universal reverse primer mix for miRNA targets (supplemental Table 1). Data were acquired using a LightCycler 480 II (Roche). Data were analyzed in Microsoft Excel 2013 (Microsoft, Redmond WA) using the geNorm method (49) and plotted in Prism v5.01 (GraphPad Software, La Jolla, CA).

Immunization—To assess effector responses, 10- to 12-week-old naïve wild-type and miR-$191^{f/f}$LckCre$^+$ mice were immunized subcutaneously on the left distal flank with 200 μl of an emulsion containing 10 μg of ovalbumin$_{257-264}$ (OT-I) and 10 μg ovalbumin$_{323-339}$ (OT-II) peptides (InvivoGen, San Diego, CA) in DPBS and complete Freund adjuvant (Sigma-Aldrich). Seven days later, the spleen and lymph nodes were collected for flow cytometric analysis. Antigen-specific responses were assessed by pulsing 1 $\times$ 10^6 total splenocytes and lymphocytes with 10 μM OT-I or OT-II peptides. Cells were plated at 5 $\times$ 10^6 cells/ml in U-bottom plates and cultured in complete RPMI in the presence of 3 μg/ml brefeldin A (eBioscience) for 5 h.

In Vitro Homeostatic Survival Assay—Naïve $CD8^+$ ($CD8\beta^+$ $CD44^-CD62L^+$), central memory $CD8^+$ ($CD8\beta^+CD44^+$ $CD62L^+$), and regulatory ($CD4^+CD25^+$) T cells were purified by FACS at the Duke Flow Cytometry Shared Resource. All cells were plated at 5 $\times$ 10^5 cells/ml. $CD8^+$ cells in U-bottom plates and regulatory T cells in flat-bottom plates were precoated as in the plate-bound stimulation assay described above. At plating, naïve $CD8^+$ T cells received 1 ng/ml hIL-7 (Peprotech), memory $CD8^+$ T cells received 10 ng/ml hIL-15 (Peprotech), and regulatory T cells received 10 ng/ml hIL-2 (Peprotech). Survival was assayed by flow cytometry 72 h after plating.

miRNA-targeting Luciferase Assay—The full-length 3′ UTR of mouse Irs1 (containing the miR-191 target site) was amplified from cDNA generated from mouse $CD8^+$ T cells and

cloned into the pmiRGLO Dual-Luciferase vector (Promega, Madison, WI) downstream of firefly luciferase. A mutated version of the Irs1 3′ UTR was generated by replacing the miR-191 target site with the restriction enzyme site SalI by synthesizing (IDT) a fragment of the 3′ UTR containing the mutation and cloning the fragment into the previously generated vector using XhoI and ApaLI sites. Each Dual-Luciferase reporter vector, together with a mock or miR-191 overexpression vector, was co-transfected into NIH-3T3 cells (ATCC, Manassas, VA) cultured in complete DMEM as described above using Lipofectamine 2000. Cells were incubated for 48 h in a humidified 37 °C incubator with 5% CO_2 and then lysed. Luciferase reporter activity was determined in a Dual-Luciferase reporter assay (Promega) using an Infinite 200 plate reader (Tecan, Männedorf, Switzerland).

Statistical Analysis—All data collected are included and are shown as individual data points. The significance of differences between sample means was determined using unpaired Student's *t* test with Welch's correction for unequal variances applied where appropriate as determined using the F test.

Author Contributions—Conceptualization, E. A. L. and Q. J. L.; Methodology, E. A. L.; Investigation, E. A. L.; Validation, E. A. L.; Formal Analysis, E. A. L.; Writing, E. A. L. and Q. J. L.; Visualization, E. A. L.; Supervision, Q. J. L.

References

1. von Boehmer, H., and Hafen, K. (1993) The life span of naive α/β T cells in secondary lymphoid organs. *J. Exp. Med.* **177,** 891–896
2. Tough, D. F., and Sprent, J. (1994) Turnover of naive- and memory-phenotype T cells. *J. Exp. Med.* **179,** 1127–1135
3. Kirberg, J., Berns, A., and von Boehmer, H. (1997) Peripheral T cell survival requires continual ligation of the T cell receptor to major histocompatibility complex-encoded molecules. *J. Exp. Med.* **186,** 1269–1275
4. Schluns, K. S., Kieper, W. C., Jameson, S. C., and Lefrançois, L. (2000) Interleukin-7 mediates the homeostasis of naive and memory CD8 T cells *in vivo*. *Nat. Immunol.* **1,** 426–432
5. Zou, T., Satake, A., Corbo-Rodgers, E., Schmidt, A. M., Farrar, M. A., Maltzman, J. S., and Kambayashi, T. (2012) Cutting edge: IL-2 signals determine the degree of TCR signaling necessary to support regulatory T cell proliferation *in vivo*. *J. Immunol.* **189,** 28–32
6. Murali-Krishna, K., Lau, L. L., Sambhara, S., Lemonnier, F., Altman, J., and Ahmed, R. (1999) Persistence of memory CD8 T cells in MHC class I-deficient mice. *Science* **286,** 1377–1381
7. Becker, T. C., Wherry, E. J., Boone, D., Murali-Krishna, K., Antia, R., Ma, A., and Ahmed, R. (2002) Interleukin 15 is required for proliferative renewal of virus-specific memory CD8 T cells. *J. Exp. Med.* **195,** 1541–1548
8. Goldrath, A. W., Sivakumar, P. V., Glaccum, M., Kennedy, M. K., Bevan, M. J., Benoist, C., Mathis, D., and Butz, E. A. (2002) Cytokine requirements for acute and basal homeostatic proliferation of naive and memory CD8+ T cells. *J. Exp. Med.* **195,** 1515–1522
9. Buckley, R. H. (2000) Advances in the understanding and treatment of human severe combined immunodeficiency. *Immunol. Res.* **22,** 237–251
10. Lee, R. C., Feinbaum, R. L., and Ambros, V. (1993) The *C. elegans* heterochronic gene lin-4 encodes small RNAs with antisense complementarity to lin-14. *Cell* **75,** 843–854
11. Wightman, B., Ha, I., and Ruvkun, G. (1993) Posttranscriptional regulation of the heterochronic gene lin-14 by lin-4 mediates temporal pattern formation in *C. elegans*. *Cell* **75,** 855–862
12. Li, Q. J., Chau, J., Ebert, P. J., Sylvester, G., Min, H., Liu, G., Braich, R., Manoharan, M., Soutschek, J., Skare, P., Klein, L. O., Davis, M. M., and Chen, C. Z. (2007) miR-181a is an intrinsic modulator of T cell sensitivity and selection. *Cell* **129,** 147–161
13. Curtale, G., Citarella, F., Carissimi, C., Goldoni, M., Carucci, N., Fulci, V., Franceschini, D., Meloni, F., Barnaba, V., and Macino, G. (2010) An emerging player in the adaptive immune response: microRNA-146a is a modulator of IL-2 expression and activation-induced cell death in T lymphocytes. *Blood* **115,** 265–273
14. Jiang, S., Li, C., Olive, V., Lykken, E., Feng, F., Sevilla, J., Wan, Y., He, L., and Li, Q. J. (2011) Molecular dissection of the miR-17–92 cluster's critical dual roles in promoting Th1 responses and preventing inducible Treg differentiation. *Blood* **118,** 5487–5497
15. O'Connell, R. M., Kahn, D., Gibson, W. S., Round, J. L., Scholz, R. L., Chaudhuri, A. A., Kahn, M. E., Rao, D. S., and Baltimore, D. (2010) MicroRNA-155 promotes autoimmune inflammation by enhancing inflammatory T cell development. *Immunity* **33,** 607–619
16. Lu, L. F., Boldin, M. P., Chaudhry, A., Lin, L. L., Taganov, K. D., Hanada, T., Yoshimura, A., Baltimore, D., and Rudensky, A. Y. (2010) Function of miR-146a in controlling Treg cell-mediated regulation of Th1 responses. *Cell* **142,** 914–929
17. Lin, R., Chen, L., Chen, G., Hu, C., Jiang, S., Sevilla, J., Wan, Y., Sampson, J. H., Zhu, B., and Li, Q. J. (2014) Targeting miR-23a in CD8+ cytotoxic T lymphocytes prevents tumor-dependent immunosuppression. *J. Clin. Invest.* **124,** 5352–5367
18. Kuchen, S., Resch, W., Yamane, A., Kuo, N., Li, Z., Chakraborty, T., Wei, L., Laurence, A., Yasuda, T., Peng, S., Hu-Li, J., Lu, K., Dubois, W., Kitamura, Y., Charles, N., *et al.* (2010) Regulation of microRNA expression and abundance during lymphopoiesis. *Immunity* **32,** 828–839
19. Masuda, K., Kakugawa, K., Nakayama, T., Minato, N., Katsura, Y., and Kawamoto, H. (2007) T cell lineage determination precedes the initiation of TCR β gene rearrangement. *J. Immunol.* **179,** 3699–3706
20. Marshall, H. D., Chandele, A., Jung, Y. W., Meng, H., Poholek, A. C., Parish, I. A., Rutishauser, R., Cui, W., Kleinstein, S. H., Craft, J., and Kaech, S. M. (2011) Differential expression of Ly6C and T-bet distinguish effector and memory Th1 CD4+ cell properties during viral infection. *Immunity* **35,** 633–646
21. Cerwenka, A., Carter, L. L., Reome, J. B., Swain, S. L., and Dutton, R. W. (1998) *In vivo* persistence of CD8 polarized T cell subsets producing type 1 or type 2 cytokines. *J. Immunol.* **161,** 97–105
22. Goldrath, A. W., Bogatzki, L. Y., and Bevan, M. J. (2000) Naive T cells transiently acquire a memory-like phenotype during homeostasis-driven proliferation. *J. Exp. Med.* **192,** 557–564
23. Moriggl, R., Topham, D. J., Teglund, S., Sexl, V., McKay, C., Wang, D., Hoffmeyer, A., van Deursen, J., Sangster, M. Y., Bunting, K. D., Grosveld, G. C., and Ihle, J. N. (1999) Stat5 is required for IL-2-induced cell cycle progression of peripheral T cells. *Immunity* **10,** 249–259
24. Snow, J. W., Abraham, N., Ma, M. C., Herndier, B. G., Pastuszak, A. W., and Goldsmith, M. A. (2003) Loss of tolerance and autoimmunity affecting multiple organs in STAT5A/5B-deficient mice. *J. Immunol.* **171,** 5042–5050
25. Friedman, R. C., Farh, K. K., Burge, C. B., and Bartel, D. P. (2009) Most mammalian mRNAs are conserved targets of microRNAs. *Genome Res.* **19,** 92–105
26. Backer, J. M., Myers, M. G., Jr., Shoelson, S. E., Chin, D. J., Sun, X. J., Miralpeix, M., Hu, P., Margolis, B., Skolnik, E. Y., and Schlessinger, J. (1992) Phosphatidylinositol 3′-kinase is activated by association with IRS-1 during insulin stimulation. *EMBO J.* **11,** 3469–3479
27. Skolnik, E. Y., Lee, C. H., Batzer, A., Vicentini, L. M., Zhou, M., Daly, R., Myers, M. J., Jr., Backer, J. M., Ullrich, A., and White, M. F. (1993) The SH2/SH3 domain-containing protein GRB2 interacts with tyrosine-phosphorylated IRS1 and Shc: implications for insulin control of ras signalling. *EMBO J.* **12,** 1929–1936
28. Johnston, J. A., Wang, L. M., Hanson, E. P., Sun, X. J., White, M. F., Oakes, S. A., Pierce, J. H., and O'Shea, J. J. (1995) Interleukins 2, 4, 7, and 15 stimulate tyrosine phosphorylation of insulin receptor substrates 1 and 2 in T cells: potential role of JAK kinases. *J. Biol. Chem.* **270,** 28527–28530
29. Sun, X. J., Miralpeix, M., Myers, M. G., Jr, Glasheen, E. M., Backer, J. M., Kahn, C. R., and White, M. F. (1992) Expression and function of IRS-1 in insulin signal transmission. *J. Biol. Chem.* **267,** 22662–22672

30. Sharfe, N., and Roifman, C. M. (1997) Differential association of phosphatidylinositol 3-kinase with insulin receptor substrate (IRS)-1 and IRS-2 in human thymocytes in response to IL-7. *J. Immunol.* **159,** 1107–1114
31. Xu, X., Sarikas, A., Dias-Santagata, D. C., Dolios, G., Lafontant, P. J., Tsai, S. C., Zhu, W., Nakajima, H., Nakajima, H. O., Field, L. J., Wang, R., and Pan, Z. Q. (2008) The CUL7 E3 ubiquitin ligase targets insulin receptor substrate 1 for ubiquitin-dependent degradation. *Mol. Cell* **30,** 403–414
32. Yao, Z., Cui, Y., Watford, W. T., Bream, J. H., Yamaoka, K., Hissong, B. D., Li, D., Durum, S. K., Jiang, Q., Bhandoola, A., Hennighausen, L., and O'Shea, J. J. (2006) Stat5a/b are essential for normal lymphoid development and differentiation. *Proc. Natl. Acad. Sci. U.S.A.* **103,** 1000–1005
33. Moriggl, R., Sexl, V., Kenner, L., Duntsch, C., Stangl, K., Gingras, S., Hoffmeyer, A., Bauer, A., Piekorz, R., Wang, D., Bunting, K. D., Wagner, E. F., Sonneck, K., Valent, P., Ihle, J. N., and Beug, H. (2005) Stat5 tetramer formation is associated with leukemogenesis. *Cancer Cell* **7,** 87–99
34. Kang, J., DiBenedetto, B., Narayan, K., Zhao, H., Der, S. D., and Chambers, C. A. (2004) STAT5 is required for thymopoiesis in a development stage-specific manner. *J. Immunol.* **173,** 2307–2314
35. Lin, J. X., Li, P., Liu, D., Jin, H. T., He, J., Ata Ur Rasheed, M., Rochman, Y., Wang, L., Cui, K., Liu, C., Kelsall, B. L., Ahmed, R., and Leonard, W. J. (2012) Critical Role of STAT5 transcription factor tetramerization for cytokine responses and normal immune function. *Immunity* **36,** 586–599
36. Henao-Mejia, J., Williams, A., Goff, L. A., Staron, M., Licona-Limón, P., Kaech, S. M., Nakayama, M., Rinn, J. L., and Flavell, R. A. (2013) The microRNA miR-181 is a critical cellular metabolic rheostat essential for NKT cell ontogenesis and lymphocyte development and homeostasis. *Immunity* **38,** 984–997
37. Rodriguez, A., Vigorito, E., Clare, S., Warren, M. V., Couttet, P., Soond, D. R., van Dongen, S., Grocock, R. J., Das, P. P., Miska, E. A., Vetrie, D., Okkenhaug, K., Enright, A. J., Dougan, G., Turner, M., and Bradley, A. (2007) Requirement of bic/microRNA-155 for normal immune function. *Science* **316,** 608–611
38. Mildner, A., Chapnik, E., Manor, O., Yona, S., Kim, K. W., Aychek, T., Varol, D., Beck, G., Itzhaki, Z. B., Feldmesser, E., Amit, I., Hornstein, E., and Jung, S. (2013) Mononuclear phagocyte miRNome analysis identifies miR-142 as critical regulator of murine dendritic cell homeostasis. *Blood* **121,** 1016–1027
39. Kramer, N. J., Wang, W. L., Reyes, E. Y., Kumar, B., Chen, C. C., Ramakrishna, C., Cantin, E. M., Vonderfecht, S. L., Taganov, K. D., Chau, N., and Boldin, M. P. (2015) Altered lymphopoiesis and immunodeficiency in miR-142 null mice. *Blood* **125,** 3720–3730
40. Guimond, M., Veenstra, R. G., Grindler, D. J., Zhang, H., Cui, Y., Murphy, R. D., Kim, S. Y., Na, R., Hennighausen, L., Kurtulus, S., Erman, B., Matzinger, P., Merchant, M. S., and Mackall, C. L. (2009) Interleukin 7 signaling in dendritic cells regulates the homeostatic proliferation and niche size of CD4+ T cells. *Nat. Immunol.* **10,** 149–157
41. Decaluwe, H., Taillardet, M., Corcuff, E., Munitic, I., Law, H. K., Rocha, B., Rivière, Y., and Di Santo, J. P. (2010) γ(c) deficiency precludes CD8+ T cell memory despite formation of potent T cell effectors. *Proc. Natl. Acad. Sci. U.S.A.* **107,** 9311–9316
42. Mitchell, D. M., and Williams, M. A. (2013) Disparate roles for STAT5 in primary and secondary CTL responses. *J. Immunol.* **190,** 3390–3398
43. Tripathi, P., Kurtulus, S., Wojciechowski, S., Sholl, A., Hoebe, K., Morris, S. C., Finkelman, F. D., Grimes, H. L., and Hildeman, D. A. (2010) STAT5 is critical to maintain effector CD8+ T cell responses. *J. Immunol.* **185,** 2116–2124
44. Metz, H. E., Kargl, J., Busch, S. E., Kim, K. H., Kurland, B. F., Abberbock, S. R., Randolph-Habecker, J., Knoblaugh, S. E., Kolls, J. K., White, M. F., and Houghton, A. M. (2016) Insulin receptor substrate-1 deficiency drives a proinflammatory phenotype in KRAS mutant lung adenocarcinoma. *Proc. Natl. Acad. Sci. U.S.A.* **113,** 8795–8800
45. Ramezani, A., Hawley, T. S., and Hawley, R. G. (2000) Lentiviral vectors for enhanced gene expression in human hematopoietic cells. *Mol. Ther.* **2,** 458–469
46. Mayr, C., and Bartel, D. P. (2009) Widespread shortening of 3′ UTRs by alternative cleavage and polyadenylation activates oncogenes in cancer cells. *Cell* **138,** 673–684
47. Tsuruzoe, K., Emkey, R., Kriauciunas, K. M., Ueki, K., and Kahn, C. R. (2001) Insulin receptor substrate 3 (IRS-3) and IRS-4 impair IRS-1- and IRS-2-mediated signaling. *Mol. Cell. Biol.* **21,** 26–38
48. Morita, S., Kojima, T., and Kitamura, T. (2000) Plat-E: an efficient and stable system for transient packaging of retroviruses. *Gene Ther.* **7,** 1063–1066
49. Vandesompele, J., De Preter, K., Pattyn, F., Poppe, B., Van Roy, N., De Paepe, A., and Speleman, F. (2002) Accurate normalization of real-time quantitative RT-PCR data by geometric averaging of multiple internal control genes. *Genome Biol.* **3,** RESEARCH0034